

TOOLBOX FOR 3D MODELLING AND IMAGE RECONSTRUCTION IN ELECTRICAL CAPACITANCE TOMOGRAPHY

Jacek Kryszyn, Waldemar Smolik

Warsaw University of Technology, Faculty of Electronics and Information Technology, The Institute of Radioelectronics and Multimedia Technology, Nuclear and Medical Electronics Division

Abstract. *Electrical Capacitance Tomography is used to visualize a spatial distribution of electric permittivity in a tomographic sensor. ECT is able to create even thousands of frames per second which is suitable for application in the industry, e.g. monitoring of multiphase flows or material mixing. A tool for sensor modelling and image reconstruction is needed in order to develop improved solutions and to better understand phenomena in ECT. A software for 2D and 2D modelling is developed in the Division of Nuclear and Medical Electronics. In this paper a Matlab toolbox called ECTsim for 3D modelling is presented.*

Keywords: electrical capacitance tomography, 3D modelling, image reconstruction

PAKIET DO TRÓJWYMIAROWEGO MODELOWANIA I REKONSTRUKCJI OBRAZÓW W ELEKTRYCZNEJ TOMOGRAFII POJEMNOŚCIOWEJ

Streszczenie. *Elektryczna tomografia pojemnościowa jest używana do obrazowania przestrzennego rozkładu przenikalności elektrycznej w sondzie tomograficznej. Elektryczna tomografia pojemnościowa pozwala uzyskać nawet kilka tysięcy obrazów na sekundę co sprawia, że znajduje zastosowanie w przemyśle, na przykład do monitorowania przepływów wielofazowych lub mieszania materiałów. Dla uzyskania lepszych rezultatów obrazowania i lepszego zrozumienia zjawisk zachodzących w elektrycznej tomografii pojemnościowej potrzebne są narzędzia do modelowania i rekonstrukcji obrazów. W Zakładzie Elektroniki Jądrowej i Medycznej rozwijane jest oprogramowanie do modelowania 2D i 3D. W artykule przedstawiono pakiet ECTsim dla środowiska Matlab do modelowania trójwymiarowego*

Słowa kluczowe: elektryczna tomografia pojemnościowa, modelowanie trójwymiarowe, rekonstrukcja obrazów

Introduction

Electrical Capacitance Tomography (ECT) is a method which is used to visualize a spatial distribution of the dielectric permittivity of objects placed inside a tomographic sensor. The image is reconstructed from measurements of mutual capacitances between electrodes placed around the examined volume [2]. It is possible to achieve even several thousand images per second with ECT. This technique has applications mainly in industrial processes like visualizing multiphase flows, mixing and stirring of materials and monitoring combustion processes [3, 7].

In the Division of Nuclear and Medical Electronics a software and hardware for ECT is being developed. The Matlab toolbox ECTsim 1.1 for 2D modelling was elaborated a decade ago. The custom finite element method implemented in this software accelerates the computations of a sensitivity matrix and enables fast nonlinear image reconstruction. For several years the ECTsim 3.0 toolbox for 3D modeling is being developed. This paper presents features and exemplary results achievable with ECTsim 3.0.

1. Challenges in ECT

1.1. Design and modelling of a 3D sensor

One of important parts of ECT system is a tomographic sensor. Parameters of the probe have an influence on quality of reconstructed images.

Usually tomographic sensors have a cylindrical or cuboidal geometry with one ring of 8 to 32 electrodes. Spatial resolution of reconstructed images depends on number of electrodes. More electrodes give better resolution but result in smaller mutual capacitances due to decreasing area of the electrodes. More precise measurement methods have to be used in order to maintain satisfactory quality of capacitance measurements [8]. Typically, in a 2D sensor which has one ring of electrodes height of the electrodes is equal to the diameter of the sensor. The pair of

adjacent electrodes has a capacitance value equal to around 1 pF whereas opposite electrodes can have a capacitance value lower by two orders of magnitude [11]. Such a wide range of measured values complicates measurement process. In order to decrease capacitance value between adjacent electrodes it is possible to insert electric screens between them. Sensors with one ring of electrodes are characterized with poor resolution in z axis due to large height of electrodes. A sensor with more than one ring of electrodes allows to measure capacitances needed to reconstruct three dimensional images. In such case measurements are performed between electrodes in all rings. To further increase resolution in 3D sensors it is possible to apply solution called “wobbling” in CT: shifting rings by half of electrodes’ width.

To limit influence of external electrical field a sensor has to be isolated with an electric screen which wraps the sensor around. Additionally, guard electrodes above and below rings of electrodes can be added to minimize influence of objects placed near opened boundaries of the sensor. The guard electrodes can be set to zero potential or can be excited synchronously with application electrodes. Fig. 1 shows lines of electric field in a sensor without and with guard electrodes.

Electrodes in a tomographic sensor can be placed on the outer side of the wall of the sensor, on the inner side of the wall of the sensor or in the wall of the sensor. In case of external electrodes, the construction of such a sensor is simple. Measurement process is not invasive because electrodes do not interact with measured material. Moreover, electrodes do not corrode because of that fact. Downside of such a solution is that the wall of the sensor modifies the field of view of the electrodes and makes measurements less linear. The better solution is to have internal electrodes which is much harder to implement because of required isolation.

To enable 3D measurements, the size of electrodes has to decrease. This means that methods of measuring small capacitances have to improve. It is also important to be able to model tomographic sensors in order to simulate mutual capacitance values between electrodes which can be used to evaluate usefulness of such a sensor.

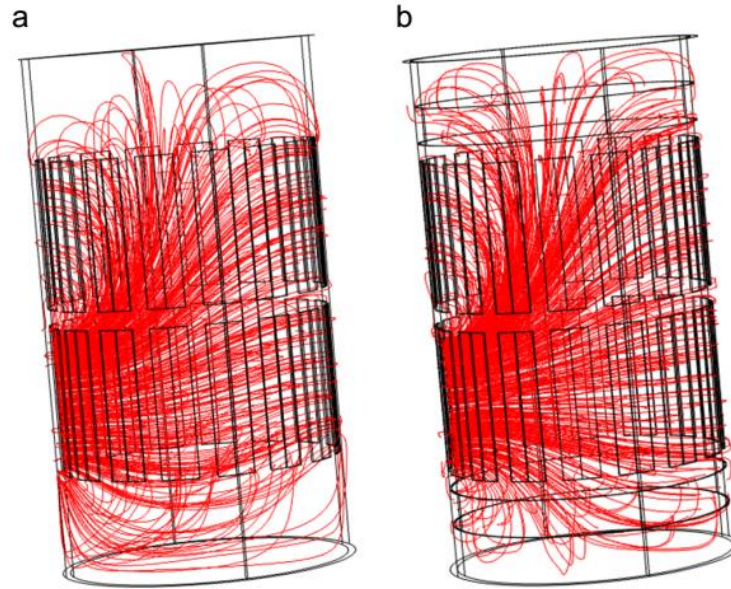


Fig. 1. Tomographic sensor with 4 rings of 8 electrodes each and electric field lines inside the sensor a) without guard electrodes; b) with guard electrodes

1.2. Image reconstruction

One of main challenges in ECT is image reconstruction. A number of independent measurements is lower (sometimes even by an order of magnitude) than a number of pixels in reconstructed image. Additionally, the sensitivity of capacitance measurement on permittivity change in a small volume is very low especially in the center of the sensor. This means that the inverse problem in ECT is ill-posed and numerically ill-conditioned [4]. Three dimensional calculations result in even worse conditioned problem. That is why there is a need for a toolbox which allows efficient image reconstruction with nonlinear, regularized methods [5]. In the nonlinear approach the challenge is that a sensitivity matrix has to be recalculated in every step which can be time consuming in case of 3D image reconstruction.

2. ECTsim 3.0

ECT 3.0 is a software for three-dimensional modelling and image reconstruction in electrical capacitance tomography designed for Matlab environment [1]. It allows to:

- create a model of the cylindrical sensor with one or more rings of electrodes,
- create a model of a phantom,
- simulate a distribution of electric field in the sensor,
- calculate sensitivity matrix for the model,
- calculate values of mutual capacitance between electrodes,
- reconstruct image from simulated or measured data,
- visualize models and calculated data in order to allow qualitative assessment of simulations.

All models are three dimensional and are built with a regular cubic mesh. In order to avoid so called inverse crime, the forward problem is calculated in a high density mesh while the image reconstruction uses a coarse mesh.

ECTsim 3.0 is an object oriented toolbox. It consists of the following classes:

- *eSet* class – represents sensors and phantoms as a set of primitive shapes;
- *eSphere* – a primitive's shape – a sphere;
- *eCylinder* – a primitive shape – a cylinder;
- *eCuboid* – one of primitive shape – a cuboid;
- *eMaterial* – a material from which the shape is built characterized by electrical permittivity;
- *phantom_generator* – a graphical generator of phantoms consisting of PVC rods placed in hexagonal nodes;

- *eModel* – represents a model of the sensor and the phantom; contains methods for 2D and 3D data visualization;
- *eCube_Mesh* – generate a cubical mesh. Interpolates the data if model elements are thinner than discrete element size. Contains linear and Cartesian coordinates of mesh points;
- *eElectrical_Field* – calculates the distribution of electric field in the model;
- *eFwd_Problem* – represents the forward problem; allows to calculate 3D sensitivity matrix and mutual capacitances;
- *eInv_Problem* – represents the inverse problem. To implement a reconstruction algorithm a class which inherits from *eInv_Problem* has to be created;
- *eInv_Problem_LBP* – a class which inherits from *eInv_Problem* and reconstructs images with the LBP algorithm (one step linear back projection);
- *eInv_Problem_Landweber* – a class which inherits from *eInv_Problem* and reconstructs images with the Landweber algorithm (a simplified gradient method); a user can adjust parameters like number of iterations, length of step, stop condition.

In order to calculate the distribution of electric field a cell method is used which uses integral form of Maxwell equations [6, 9]. Because of this there is no need to calculate second order derivatives (no divergence or rotation).

In case of a cubical mesh every element has 6 neighbours. Coordinates of elements are noted with (i, j, k) . In each element the electrical permittivity and the potential are constant. Electrical field in each element is described with an equation:

$$\sum_{l=1}^6 \varepsilon_l \nabla \varphi_l \cdot \vec{ds} = \sum_{l=1}^6 \varepsilon_l \nabla \varphi_l \cdot \vec{n}_l h_l = 0 \quad (1)$$

where ε_l is an arithmetic average of permittivity of a given element and its current neighbour, h_l is a size of the grid and φ_l is a potential in the element. If

$$\nabla \varphi_l \cdot \vec{n}_l = \frac{\varphi_{i,j,k} - \varphi_{i+\Delta i, j+\Delta j, k+\Delta k}}{h_l} \quad (2)$$

and $h_l = 1$, then the equation for the potential in the element is

$$\varphi_{i,j,k} = \frac{\sum_{m=-1,1} \varphi_{i+m,j,k} (\varepsilon_{i+m,j,k} + \varepsilon_{i,j,k}) + \sum_{n=-1,1} \varphi_{i,j+n,k} (\varepsilon_{i,j+n,k} + \varepsilon_{i,j,k})}{6\varepsilon_{i,j,k} + \varepsilon_{i+1,j,k} + \varepsilon_{i-1,j,k} + \varepsilon_{i,j+1,k} + \varepsilon_{i,j-1,k} + \varepsilon_{i,j,k+1} + \varepsilon_{i,j,k-1}} + \frac{\sum_{l=-1,1} \varphi_{i,j,k-l} (\varepsilon_{i,j,k-l} + \varepsilon_{i,j,k})}{6\varepsilon_{i,j,k} + \varepsilon_{i+1,j,k} + \varepsilon_{i-1,j,k} + \varepsilon_{i,j+1,k} + \varepsilon_{i,j-1,k} + \varepsilon_{i,j,k+1} + \varepsilon_{i,j,k-1}} \quad (3)$$

In order to calculate the distribution of the electric field a linear system consisting of above equations for all elements has to be prepared but it would be too large (tens of GB) to put it in memory of a computer. In ECTsim 3.0 a modification of Kaczmarz iterative algorithm is used which forms an equation for one element and solves it in each step. In order to accelerate calculations a MEX file with an external procedure in C language was written.

Capacitances are calculated using the linear approximation:

$$\mathbf{C} = \mathbf{S}\boldsymbol{\varepsilon}$$

where \mathbf{C} is a mutual capacitance vector, \mathbf{S} is a sensitivity matrix and $\boldsymbol{\varepsilon}$ is a permittivity vector. In order to avoid numerical errors coming from cubical mesh the capacitance values are not calculated with Gauss law. Because of usage of cubical mesh, the electrodes of cylindrical sensor have different shapes depending of placement. A special function called *geometric_correction* was made to minimize such errors. The function ensures equality of integral sensitivity of all pairs of electrodes shifted by the same angle.

The forward problem is calculated three times: for the empty sensor, the sensor filled with material with maximum permittivity and the sensor filled with the phantom. To decrease the time needed for the calculations they can be performed simultaneously on machines with more than one core using *parfor* instruction.

In case of the inverse problem solution the uniform distribution of electric permittivity in the field of view of the sensor is used as the starting point of image reconstruction. Images are reconstructed in a low resolution grid whereas forward problem is calculated in high resolution grid so special methods for down sampling of the sensitivity matrix and permittivity distribution are provided in the *eInv_Problem* class. To reconstruct images from measured data a *get_C_from_file* method has to be used which allows to read data from ET3 tomograph in a form of a text file. Methods for evaluation of errors and image quality and errors are provided. For example, it is possible to compare a reconstructed image to a numerical model. The reconstructed images can be visualized in 2D and 3D with one of many methods provided in the *eInv_Problem* class. In the case of application of regularization in the image reconstruction, it is possible to use TSVD or Tikhonov method.

3. Example of use

3.1. Forward problem

A sensor with following parameters was modeled:

- cylindrical sensor,
- inner diameter = 153 mm,
- wall thickness = 3 mm,
- height = 250 mm,
- electric permittivity of the wall = 3 (PVC material),
- 2 rings of 16 electrodes in each ring,
- height of electrodes = 80 mm,
- width of electrodes = 20 mm,
- internal electrodes.

The sensor was modeled in two variants: without guard electrodes and with them (Fig. 2). The former was used only to present the difference in the distribution of electric field between not guarded and guarded sensor. The latter was used for further experiments. The height of guard electrodes was set to 20 mm.

The size of mesh cells was set to 4 mm in x, y and z. The numerical model consisted of 105489 cells.

Models of empty sensor from ECTsim 3.0 were compared with models created in COMSOL (Fig. 2b and Fig. 2d) in order to validate the method of the simulation used in ECTsim 3.0.

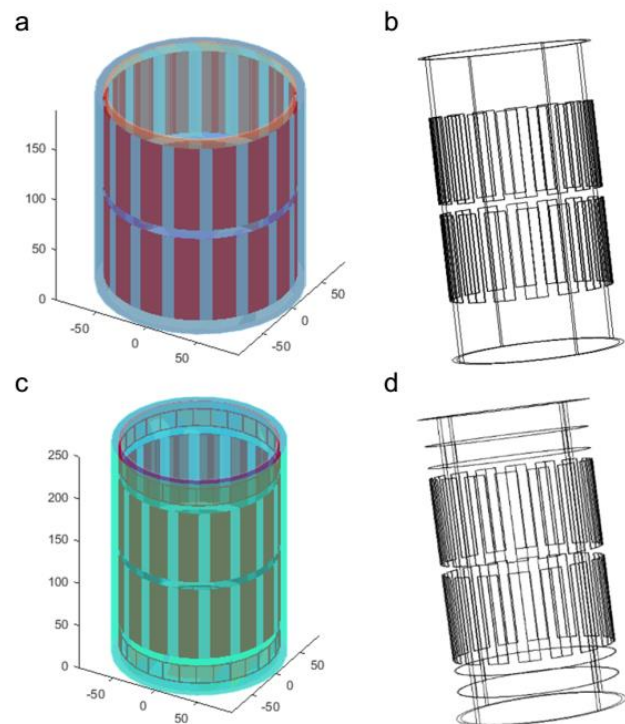


Fig. 2. Model of a sensor a) without guard electrodes; ECTsim 3.0 b) without guard electrodes; COMSOL c) with guard electrodes; ECTsim 3.0 d) COMSOL

Fig. 3 shows simulated distributions of electric field in ECTsim 3.0 and COMSOL for both variants of the sensor. *Slice* function from Matlab was used to show volumetric data in ECTsim 3.0. It is possible to see that lines of electric field in a sensor with guard screens are limited to the electrodes whereas in not guarded sensor they flow out of the sensor in z axis. Further results will only include the model with guard electrodes.

Fig. 4 shows one-dimensional cross section from two different planes (along x axis perpendicularly to the center of the excitation electrode and y axis going through the middle of the field of view) of the distribution of electric field calculated with ECTsim 3.0 and COMSOL. Results from ECTsim 3.0 and COMSOL are very close to each other. The discrepancy is due to the different interpolation used in both numerical solvers.

Figure 5 shows sensitivity maps calculated by ECTsim 3.0. The maps are presented in 2D and 3D.

Fig. 6 and Fig. 7 show mutual capacitance values between electrodes of the sensor which were numerically calculated in ECTsim 3.0 respectively in linear and logarithmic scale. First electrode was the excitation electrode (10 V) and electrodes from 2 to 32 were measurement electrodes. Capacitance values were calculated for the empty sensor (green bars) and the sensor filled with a solid material with permittivity equal to 3 (yellow bars). The highest value is over 2 orders of magnitude bigger than the lowest. This presents one of challenges of ECT which is measuring not only small values of capacitance but also values in a very wide range.

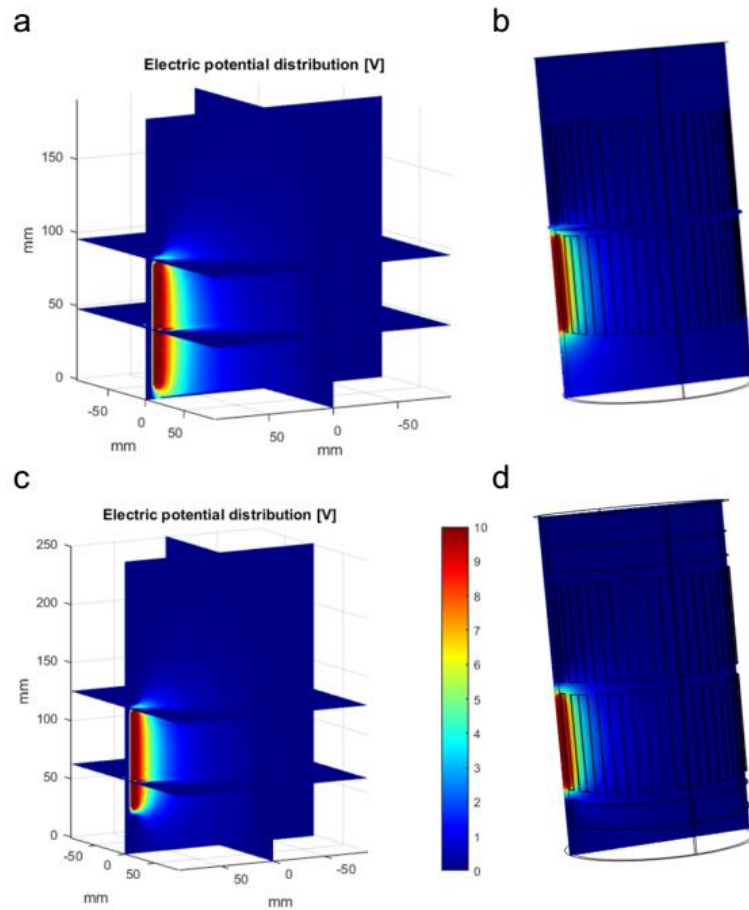


Fig. 3. Distribution of electric potential in a model without guard electrodes a) ECTsim 3.0 b) COMSOL and in a model with guard electrodes c) ECTsim 3.0 d) COMSOL

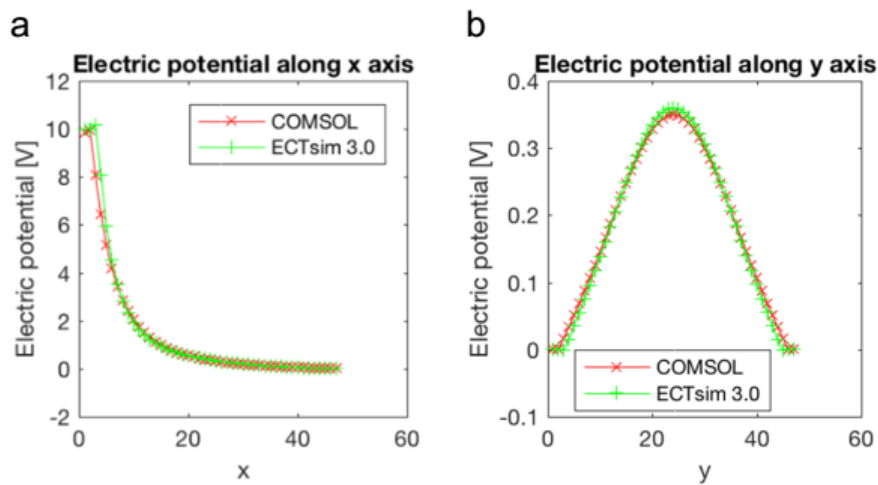


Fig. 4. Comparison of electric field calculated numerically in ECTsim 3.0 and COMSOL. Electric potential along: (a) x axis. Plane is perpendicular to the excitation electrode and goes through the middle of the electrode; (b) y axis. Plane is parallel to the excitation electrode and goes through the middle of the field of view

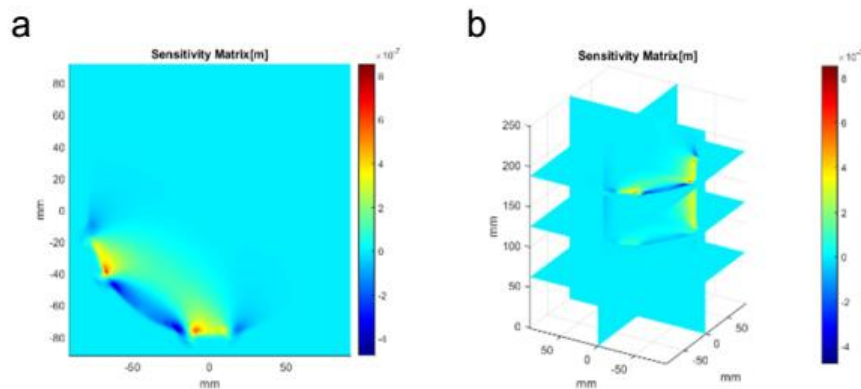


Fig. 5. Sensitivity maps calculated in ECTsim 3.0: a) 2D axial cross section; b) 3D view

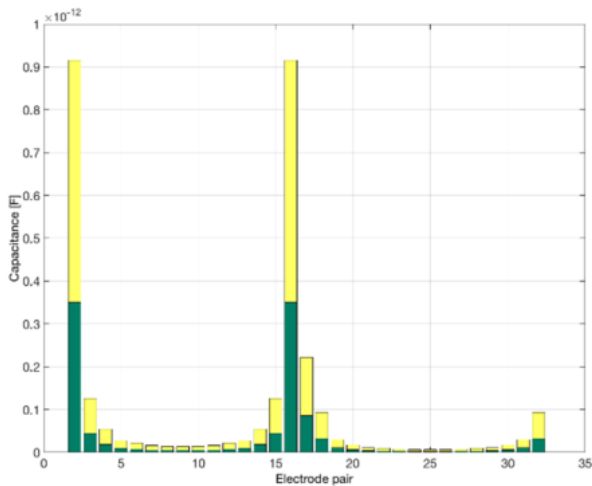


Fig. 6. Numerically calculated interelectrode capacitance. First electrode is the excitation electrode, electrodes 2-32 are measurement electrodes. Green bars represent capacitance values in the sensor filled with a low permittivity material (air). Yellow bar corresponds to capacitance values in a sensor filled with a material with relative dielectric permittivity equal to 3. Linear scale

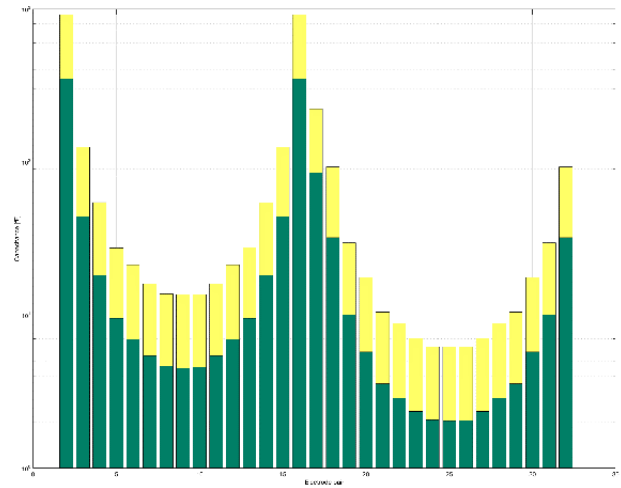


Fig. 7. Numerically calculated interelectrode capacitance. First electrode is the excitation electrode, electrodes 2-32 are measurement electrodes. Green bars represent capacitance values in a sensor filled with low permittivity material (air). Yellow bar corresponds to capacitance values in a sensor filled with a material with relative dielectric permittivity equal to 3. Logarithmic scale

3.2. Inverse problem

To compare simulated with real measurements a sensor with exact same parameters was built (Fig 8a). Electrodes from copper foil were placed inside PVC pipe. To screen the whole sensor, the pipe was wrapped with an insulator and metal screen.

A phantom consisting of four PVC rods with height equal to 40 mm was modeled. Two rods were placed in such a way that their centers were in axis with the center of lower ring of electrodes and another two were placed in a similar way, but aligned to the center of the upper ring of electrodes (Fig. 8b). A phantom corresponding to the one numerically modeled in ECTsim 3.0 was built. PVC elements were wrapped with aluminum foil in order to get a higher signal. ET3 tomograph was used for measurements. ET3 tomograph returns measured values

normalized using calibration measurements (sensor filled with air – minimum electric permittivity material and PVC beads – maximum permittivity material).

Parameters of Landweber algorithm were: 500 iterations, alfa parameter equal to 0.005.

All simulations were performed on a laptop with Intel Core i5 2.6 GHz CPU and 8 GB of RAM.

Calculation of the distribution of electric field took 553 seconds (cumulative time of simulations for the empty sensor, the sensor with the phantom and the sensor filled with solid material with electric permittivity equal to 3). Calculation of sensitivity matrices for all cases took 28.5 seconds. Calculation of the capacitances took 10.7 seconds.

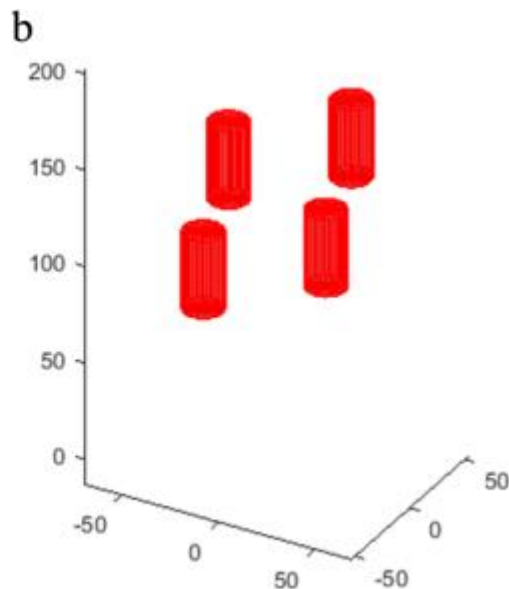


Fig. 8. a) Built sensor; b) Modelled phantom

Fig. 9 and Fig. 10 show capacitance values between electrodes in the built sensor and measured with ET3 tomograph when the first electrode was the excitation electrode and electrodes from 2 to 32 were measurement electrodes respectively in linear and logarithmic scale. Measurements were performed with the empty sensor (green bars) and the sensor filled with PVC beads which dielectric permittivity is equal to 3 (yellow bars).

Figure 11 shows image reconstruction performed with LBP algorithm using simulated capacitances. *Slice* Matlab function was used to show volumetric data. Figure 11 shows xy, xz and xy cross sections of the reconstructed 3D image. LBP algorithms performs badly – it is impossible to distinguish rods which merged into one volume.

Figure 12 shows image reconstruction performed with Landweber algorithm using simulated data. The same views as in Figure 11 were presented. The result shows that to reconstruct 3D images an iterative algorithm has to be used. All four elements are distinguished in the reconstructed image. ECTsim 3.0 allows to visualize 3D data in many ways. Fig. 13 shows 3D maximum intensity projection of the reconstructed volume.

Time of calculation was following:

- LBP algorithm – 0.84 s,
- Landweber algorithm – 35 seconds.

LBP algorithm can be used to calculate an initial solution for iterative algorithm.

Figure 14 shows image reconstruction performed with Landweber algorithm using measured data. The same views as in Figure 11 and Figure 12 were presented. It turned out that electrodes in the designed sensor were too small in order to allow capacitance measurements with ET3 tomograph which has limited sensitivity (about 10 fF). Signal to noise ratio for the smallest capacitances was too low.

Figure 15 shows the normalized capacitance error err_c in next iterations for the Landweber algorithm using the simulated data and the measured data. The error was calculated with formulas:

$$err_c = \|C_r - C_m\|$$

where C_r – reconstructed capacitance values, C_m – simulated capacitance values for the sensor with the phantom. After 500 iterations errors were following:

- $err_c - 0.001410$;
- $err_c - 0.261900$;

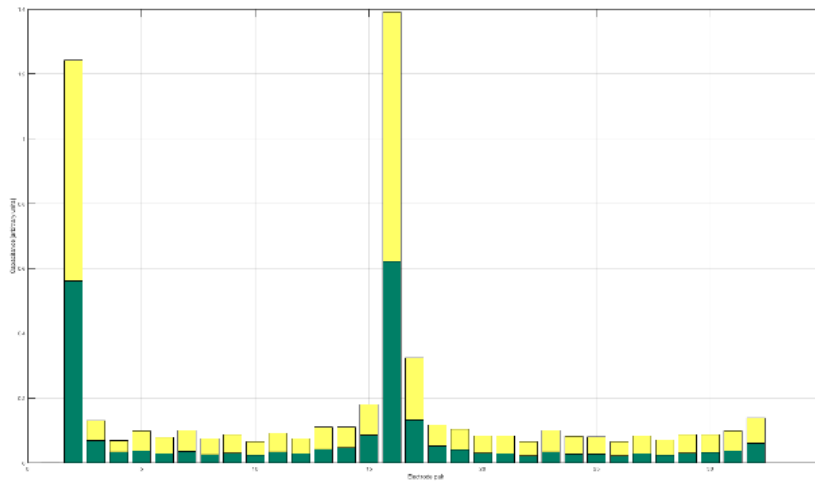


Fig. 9. Measured inter electrode capacitance values. First electrode is the excitation electrode, electrodes 2-32 are measurement electrodes. Green bars represent capacitance values in the sensor filled with a low permittivity material (air). Yellow bars correspond to capacitance values in the sensor filled with a material with relative dielectric permittivity equal to 3. Linear scale

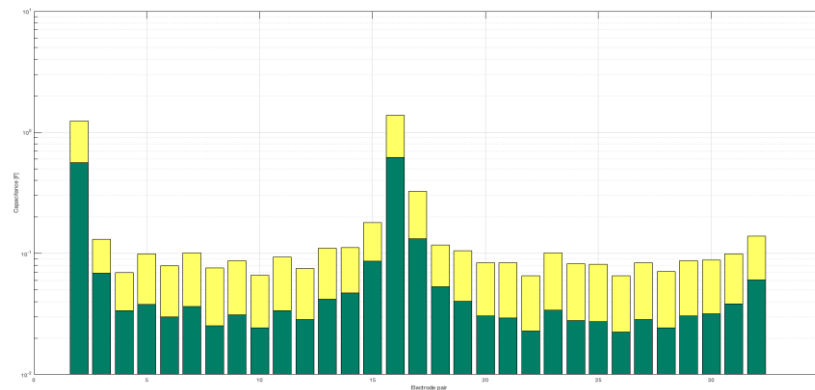


Fig. 10. Measured interelectrode capacitance values. First electrode is the excitation electrode, electrodes 2-32 are measurement electrodes. Green bars represent capacitance values in the sensor filled with a low permittivity material (air). Yellow bars correspond to capacitance values in the sensor filled with a material with relative dielectric permittivity equal to 3. Logarithmic scale

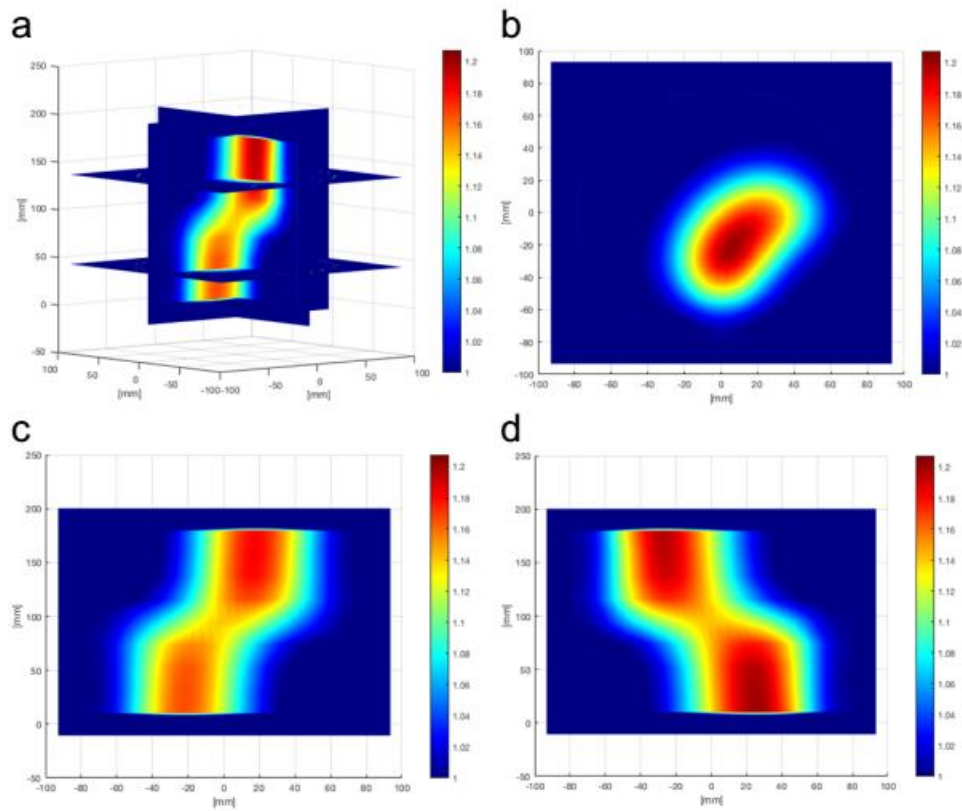


Fig. 11. LBP reconstruction from simulated capacitances: a) four planes from 3D reconstruction image; b) xy slice of the reconstructed volume; c) xz slice of the reconstructed volume; d) yz slice of the reconstructed volume

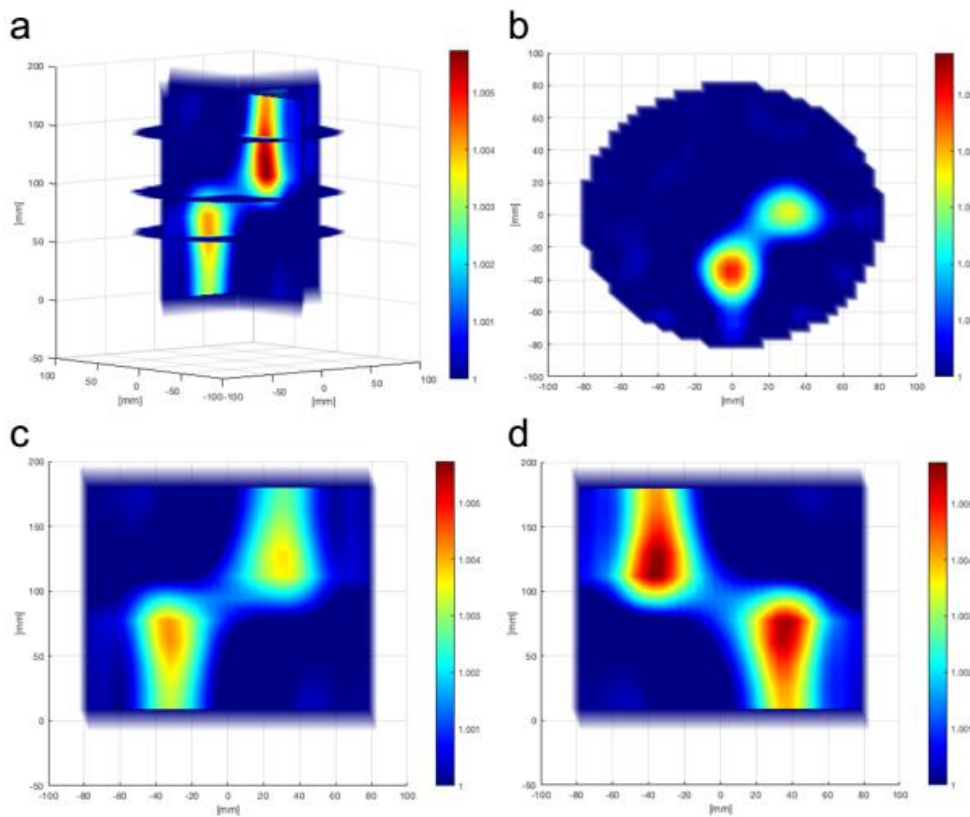


Fig. 12. Landweber reconstruction from simulated capacitances: a) four planes from 3D reconstruction image; b) xy slice of the reconstructed volume; c) xz slice of the reconstructed volume; d) yz slice of the reconstructed volume

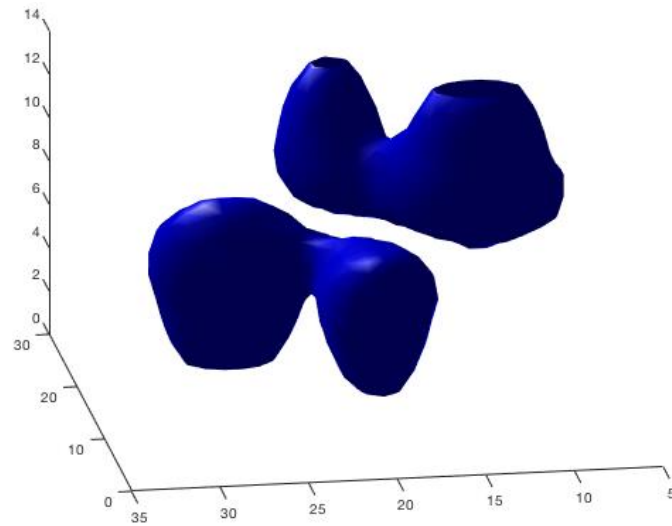


Fig. 13. 3D visualization of the phantom after the reconstruction with the Landweber algorithm

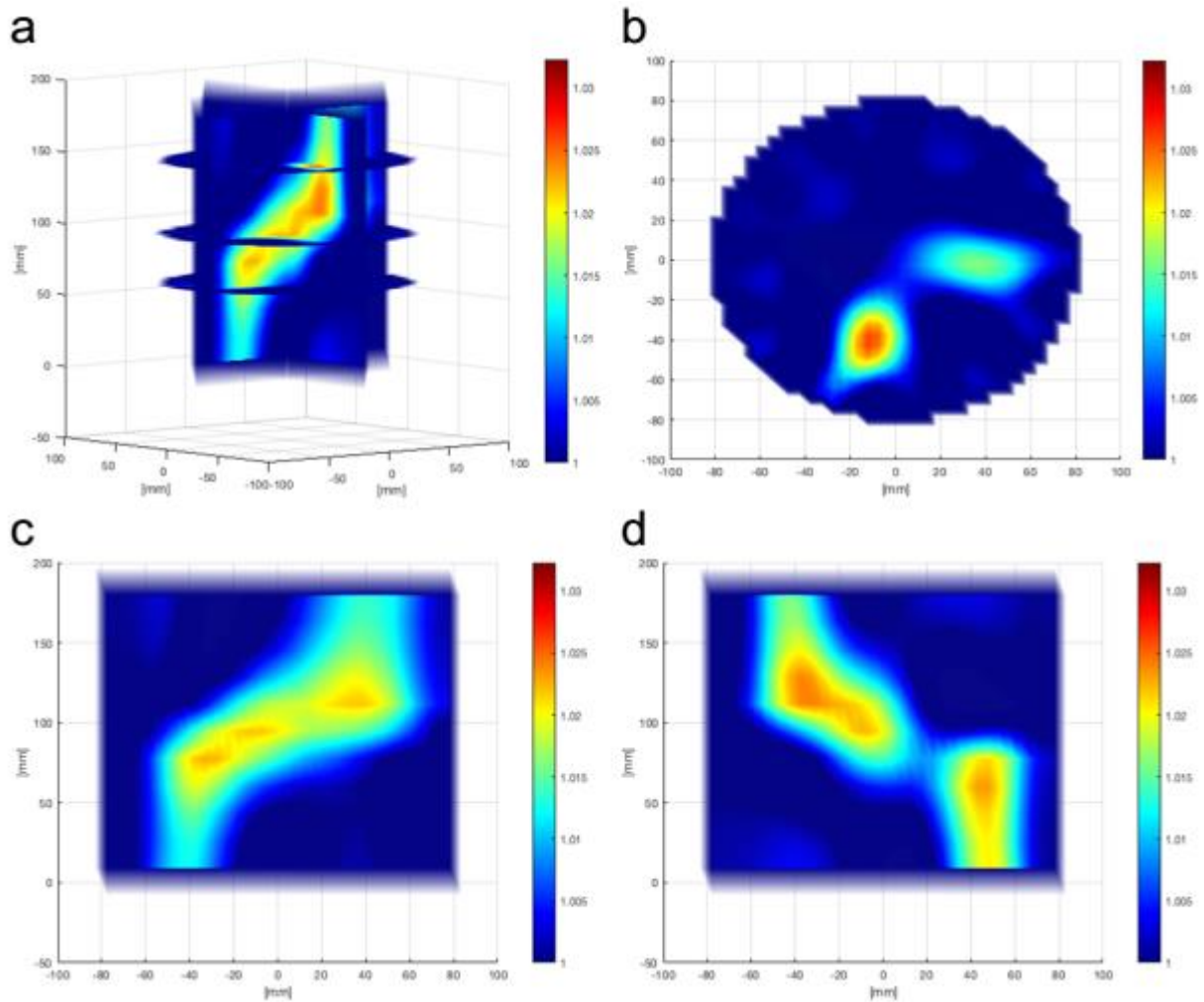


Fig. 14. Landweber reconstruction from measured capacitances: a) four planes from 3D reconstruction image; b) xy slice of the reconstructed volume; c) xz slice of the reconstructed volume; d) yz slice of the reconstructed volume

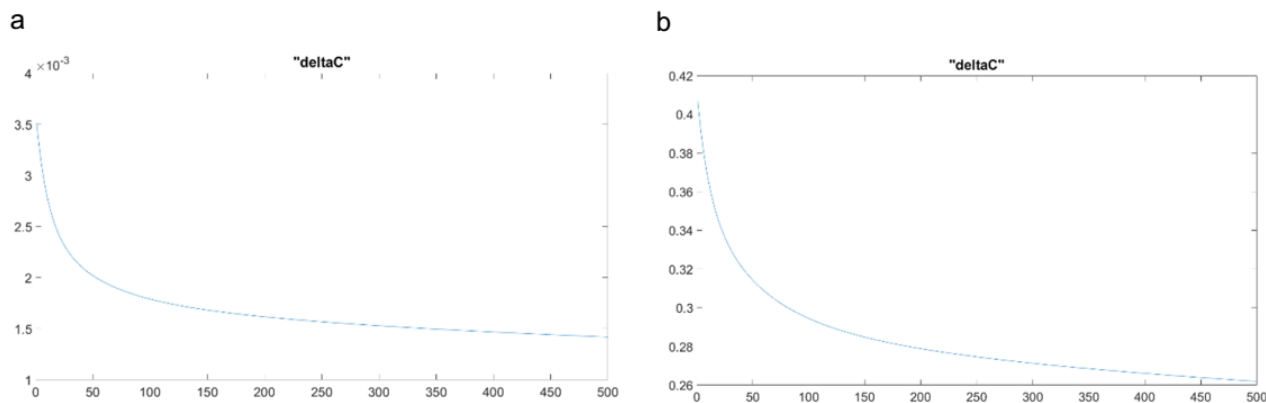


Fig. 15. Normalized capacitance error as a function of number of iterations of the Landweber algorithm: a) simulated data, b) real data

4. Conclusions

ECTsim 3.0 toolbox for modeling and image reconstruction in ECT was presented. It allows to perform 3D simulations of distribution of electric field with a precision comparable to a commercial software like COMSOL. Using ECTsim it is possible to model a sensor before constructing it in order to evaluate its parameters. Creation of a model is easy and straightforward. ECTsim 3.0 allows to calculate forward problem which results in 3D sensitivity matrix for the sensor and simulated measurements for assumed permittivity distribution in examined object. ECTsim 3.0 allows also to reconstruct images from simulated data which allows to test different reconstruction algorithms. It is also possible to reconstruct images using imported data from real tomographic system. This allows to evaluate ECT system usefulness for 3D imaging.

The main drawback of the proposed software is time needed for calculations. Forward problem is solved using an iterative algorithm due to extreme size of matrices which are produced in 3D modelling. One of the solutions of the problem could be a usage of sparse matrices and Krylov algorithms which solve linear systems using matrix-vector multiplications.

Although iterative linear reconstruction algorithm produces good quality images, it is possible to obtain better results with nonlinear algorithms. Sensitivity matrix (Jacobian) changes in every iteration in such algorithms which is computationally expensive in case of 3D image reconstruction. The solution of this problem may be an iterative algorithm which is linear in certain ranges. In [10] authors prove that it is not necessary to change sensitivity matrix in every step. Even few recalculations of sensitivity matrix may significantly improve quality of image reconstruction.

Bibliography

- [1] Bielecki K., Smolik W.: Pakiet ectsim do modelowania w elektrycznej tomografii pojemnościowej, VI Sympozjum Naukowe Techniki Przetwarzania Obrazu – TPO'2010, Serock, 2010, 106–114.
- [2] Huang S. M., Plaskowski A., Xie C. G., Beck M. S.: Capacitance-based tomographic flow imaging system. *Electron. Lett.*, 24/1988, 418–419.
- [3] Jaworski A. J., Dyakowski T.: Application of electrical capacitance tomography for measurement of gas-solid flow characteristics in a pneumatic conveying system. *Meas. Sci. Technol.*, 12/2001, 1109–1119.
- [4] Lionheart W. R.: EIT reconstruction algorithms: pitfalls, challenges and recent developments. *Physiol. Meas.*, 25/2004, 125–142.

- [5] Lionheart W., Polydorides N., Borsic A.: The reconstruction problem, *Electrical Impedance Tomography: Methods, History and Applications*, D. S. Holder, Ed., ed: Institute of Physics, 2004, 3–64.
- [6] Mirkowski J., Smolik W. T., Yang M., Olszewski T., Szabatin R., Radomski D., Yang W. Q.: A New Forward-Problem Solver Based on a Capacitor-Mesh Model for Electrical Capacitance Tomography. *IEEE Trans. Instrumentation and Measurement*, 57/2008.
- [7] Plaskowski A., Beck M., Thorn R., Dyakowski T.: *Imaging industrial flows. Applications of electrical process tomography*. IOP Publishing Ltd., 1995.
- [8] Reinecke N., Mewes D.: Recent developments and industrial research applications of capacitance tomography. *Meas. Sci. Technol.*, 7/1996., 325–337.
- [9] Smolik W.: Forward Problem Solver for Image Reconstruction by Nonlinear Optimization in Electrical Capacitance Tomography, *Flow Measurement and Instrumentation*, 21/2010, 70–77.
- [10] Smolik W., Mirkowski J., Olszewski T., Szabatin R.: Verification of image reconstruction algorithm with sensitivity matrix updating for real data in electrical capacitance tomography. *Proc. 4th International Symposium on Process Tomography in Poland, Warsaw, Poland, 2006*.
- [11] Yang W. Q.: Hardware design of electrical capacitance tomography systems. *Meas. Sci. Technol.*, 7/1996, 225–232.

M.Sc. Jacek Kryszyn

e-mail: j.kryszyn@ire.pw.edu.pl

Received the M. Sc. degree in electronics and computer engineering from Warsaw University of Technology, Warsaw, Poland in 2012. PhD student and the Assistant with the Nuclear and Medical Electronics Division, Institute of Radioelectronics, Electronics and Information Technology Faculty, Warsaw University of Technology. His field of interest covers Electrical Capacitance Tomography, especially simulations of the electric field and reconstruction of images.



Ph.D. Eng. Waldemar T. Smolik

e-mail: w.smolik@ire.pw.edu.pl

Waldemar T. Smolik received the M.Sc., the Ph.D. and D.Sc. degree in electronics engineering from Warsaw University of Technology, Warsaw, Poland in 1991, 1997 and 2014, respectively. Since 2014, he is an Associate Professor at the Institute of Radioelectronics and Multimedia Technology, Electronics and Information Technology Faculty, Warsaw University of Technology. He is the head of the Laboratory of Electronics Application in Nuclear Medicine at the Division of Nuclear and Medical Electronics. His main research interests are computer engineering, computed tomography and medical imaging. He has published over 70 scientific papers.



otrzymano/received: 20.09.2016

przyjęto do druku/accepted: 15.02.2017